The Astronomical Journal, 155:158 (11pp), 2018 April https://doi.org/10.3847/1538-3881/aaaeb6

Validation and Initial Characterization of the Long-period Planet Kepler-1654 b

C. A. Beichman[1], H. A. C. Giles[2], R. Akeson[1], D. Ciardi[1], J. Christiansen[1], H. Isaacson[3], G. M. Marcy[3], E. Sinukoff[4], T. Greene[5], J. J. Fortney[6], I. Crossfield[7], R. Hu[8], A. W. Howard[9], E. A. Petigura[9], and H. A. Knutson[9]
[1] NASA Exoplanet Science Institute and Infrared Processing and Analysis Center, California Institute of Technology, Jet Propulsion Laboratory, Pasadena, CA 91125, USA
[2] Observatoire Astronomique de l'Université de Genève, Switzerland
[3] University of California at Berkeley, Berkeley, CA, USA
[4] Institute for Astronomy, University of Hawaii, 2680 Woodlawn Drive, Honolulu, HI 96822, USA
[5] NASA Ames Research Center, Mountain View, CA 94035, USA
[6] University of California Santa Cruz, 1156 High Street, Santa Cruz, CA 95064, USA
[7] Massachusetts Institute of Technology, 77 Massachusetts Avenue, Cambridge, MA 02139, USA
[8] Jet Propulsion Laboratory, California Institute of Technology, 4800 Oak Grove Drive, Pasadena, CA 91125, USA
[9] California Institute of Technology, 1200 East California Boulevard, Pasadena, CA 91125, USA
Received 2017 December 27; revised 2018 January 29; accepted 2018 February 8; published 2018 March 20

Abstract

Fewer than 20 transiting *Kepler* planets have periods longer than one year. Our early search of the *Kepler* light curves revealed one such system, Kepler-1654b (originally KIC 8410697b), which shows exactly two transit events and whose second transit occurred only five days before the failure of the second of two reaction wheels brought the primary *Kepler* mission to an end. A number of authors have also examined light curves from the *Kepler* mission searching for long-period planets and identified this candidate. Starting in 2014 September, we began an observational program of imaging, reconnaissance spectroscopy, and precision radial velocity (RV) measurements that confirm with a high degree of confidence that Kepler-1654b is a *bona fide* transiting planet orbiting a mature G5V star ($T_{\rm eff} = 5580$ K, $[{\rm Fe/H}] = -0.08$) with a semimajor axis of 2.03 au, a period of 1047.84 days, and a radius of 0.82 ± 0.02 $R_{\rm Jup}$. RV measurements using Keck's HIRES spectrometer obtained over 2.5 years set a limit to the planet's mass of <0.5 (3σ) $M_{\rm Jup}$. The bulk density of the planet is similar to that of Saturn or possibly lower. We assess the suitability of temperate gas giants like Kepler-1654b for transit spectroscopy with the *James Webb Space Telescope*, as their relatively cold equilibrium temperatures ($T_{\rm pl} \sim 200$ K) make them interesting from the standpoint of exoplanet atmospheric physics. Unfortunately, these low temperatures also make the atmospheric scale heights small and thus transmission spectroscopy challenging. Finally, the long time between transits can make scheduling *JWST* observations difficult—as is the case with Kepler-1654b.

Key words: planetary systems – planets and satellites: detection

1. Introduction

The *Kepler* mission (Borucki et al. 2010) has revolutionized our understanding of exoplanets, finding over 2300 confirmed planets and almost 4500 candidates[10] (Batalha et al. 2013). These data have improved our knowledge of the constituents of the inner solar system with an inventory that includes planets ranging from less than an Earth radius (Kepler 37b) up to 1.5 Jupiter radii (Kepler 12b), and periods ranging from less than a day (Kepler 78b) up to 1100 days, including Kepler 167 (Kipping et al. 2016) and Kepler 1647 (Kostov et al. 2016). A number of non-transiting *Kepler* planets with longer periods were identified by their radial velocity (RV) signature, e.g., Kepler 407c with a period of order 3000 days (Marcy et al. 2014). The completeness of the *Kepler* catalog is poor for long-period planets. These objects are hard to find a priori, as the transit probability decreases with increasing semimajor axis and because fewer transits are observable in a given observing period. A smaller number of events reduces the total signal-to-noise-ratio (S/N) achievable by averaging multiple transits. Most importantly, the *Kepler* pipeline required three or more potential transits before promoting a star to become a *Kepler* Object of Interest, or KOI, worthy of further investigation. (Jenkins et al. 2010).

To avoid the *Kepler* pipeline's prohibition against planets with one or two transits, we analyzed *Kepler* light curves *not identified* with confirmed planets, *Kepler* candidates, or KOI's. As described below, this search was rewarded with the detection of a Jupiter-sized planet in a 2.87 year (1047.836 day) period orbiting a mid-G star, KIC 8410697, which we now refer to as Kepler-1654. A more complete search for long-period systems was carried out by the Planet Hunters group (Wang et al. 2015) who identified a number of systems with one and two transits. In the case of Kepler-1654, they found only the first of its two transits. Foreman-Mackey et al. (2016) identified seven new transiting systems, showing one or at most two transits, and eight long-period planets identified with known *Kepler* systems having at least one shorter period planet.

This paper describes follow-up observations of Kepler-1654 using the W. M. Keck Observatory that have allowed us to reject a variety of alternative ("false-positive") interpretations, fully characterize the host star, and set an upper limit to its mass to be less than $0.48\,M_{\rm Jup}$ (3σ). Section 2 describes the search through the *Kepler* light curves. Section 3 presents the follow-up observations of the star, and Section 4 presents the characterization of the planet. Section 5 investigates the

[10] As of December 2107 for *Kepler* with an additional 170 confirmed planets for K2, http://exoplanetarchive.ipac.caltech.edu/.

prospects of studying the planet's atmosphere with *JWST* transit spectroscopy.

2. Searching Non-KOI Light Curves

The data used for this investigation were drawn from Quarters 1–17 and encompassed the entire duration of the *Kepler* prime mission. A total of 11232 stars were selected on the basis of their properties in the *Kepler* Stellar Database (Brown et al. 2011): *Kepler* magnitude, Kpmag <14 mag, effective temperatures between 5500 and 6000 K, and $\log g > 3.75$. These stellar values are of course only rough estimates (Huber et al. 2014) and were used only for an initial selection of likely F5-G5 dwarf stars. Data within each Quarter, $I(t)$, were normalized to near-unity using a trimmed mean signal for the entire Quarter and then searched for individual flux dips using a zero-sum Box Car filter of length $3L$ where L was allowed to range in duration from 4 to 24 hr. A local trimmed average and standard deviation were evaluated within each segment with the filter output, $S(t)$, at a given time, t, having a value,

$$S(t) = \langle I(t)\rangle_{-L/2}^{L/2} - 0.5 \times (\langle I(t)\rangle_{-3L/2}^{-L/2} + \langle I(t)\rangle_{+L/2}^{+3L/2}). \quad (1)$$

Negative going dips with S/N > 20 were output for subsequent analysis. The noise per sample, σ used in this calculation was derived on a Quarter-by-Quarter basis using a robust estimate of standard deviation of all points within the Quarter,[11] σ_Q, rejecting values deviating by more than $\pm 3\sigma$ from the initial mean and standard deviation. The S/N of a potential transit event was evaluated by dividing the depth of the event by the noise per sample, σ, and multiplying by $\sqrt{N_L}$ where N_L is the number of samples in a segment of length L.

A list of 24 systems was examined more closely. For most of the single transit cases, the transit duration combined with the approximate properties of the star yielded predicted orbital periods (Seager & Mallén-Ornelas 2003) much greater than duration of the *Kepler* mission. These systems would be impossible to confirm. In a few cases, the predicted orbital periods were short compared to the mission duration, implying that the *Kepler* pipeline should have found and considered the object if real.

One object we identified is Kepler-1654, a mid-G dwarf star with a *Kepler* magnitude of 13.42 mag, a transit depth of 0.51%, and a period of 1047.8356 days (2.87 year, Table 1). Wang et al. (2015) identified this object as having only a single transit on Day 542+2454833 (BJD). By going to the very end of Q17, we were able to identify the second transit at Day 1590 +2454833 (BJD). Foreman-Mackey et al. (2016) also found two transits for this system.

Figure 1 shows light curves from Quarters 6 and 17, which were normalized and detrended using either a linear (Q6) or 2nd order (Q17) baseline to remove small trends. We also examined the entire light curve looking for other transit signatures using the LombScargle tool available at the Exoplanet Archive.[12] No significant periodicities indicative of shorter period planets could be identified in the periodogram. A search through the *Kepler* light curve using the TERRA software (Petigura 2015) revealed no other planets in this system. This limit is approximated by a limiting depth of 80 ppm × (Period/1 day)$^{0.6}$. Thus, >80 ppm transits with one-day orbital periods ($\sim 1\,R_\oplus$) are ruled out and 100-day planets with depths >1300 ppm ($\sim 0.35\,R_{\rm Jup}$) are also ruled out. We also did not find any evidence of a transit at half of the nominal 1047.8-day period, thereby ruling out the presence of an eclipsing binary in an edge-on, circular orbit (Santerne et al. 2013).

Superimposed on the light curves in Figure 1 is a model transit curve fitted to the data as described in Section 4.1. But before describing the result of the light curve analysis, we first discuss the observations used to reject false-positive interpretations and to characterize more fully the star and the transiting planet.

Table 1
Observed Properties of Kepler-1654

Property	Value	Comment
Kepler#	1654	⋯
KIC #	8410697	⋯
2MASS designation	J18484459+4426041	⋯
α	$18^h48^m44\overset{s}{.}6$	J2000
δ	$44^d26^m04\overset{s}{.}1$	J2000
Kepler Mag	13.42	mag
J	12.28 ± 0.021	mag
H	11.93 ± 0.019	mag
K	11.92 ± 0.015	mag
WISE W1	11.88 ± 0.023	mag
WISE W2	11.92 ± 0.022	mag
$T_{\rm eff}$	5580 ± 70 K	Keck HIRES
log g	4.19 ± 0.06	Keck HIRES
[Fe/H]	−0.08 ± 0.06	Keck HIRES
Vsini	<2.0 km s^{-1}	Keck HIRES
Stellar Age	>5 Gyr	Keck HIRES

3. Follow-up Observations of Kepler-1654 and Kepler-1654b

3.1. Keck AO Imaging

We obtained near-infrared adaptive optics images of Kepler-1654 at Keck Observatory on the night of 2015 August 21 UT (Figure 2). Observations were obtained with the 1024 × 1024 NIRC2 array and the natural guide star system; the target star was bright enough to be used as the guide star. The data were acquired using the narrow-band Br-γ filter using the narrow camera field of view with a pixel scale of 9.942 mas pixel^{-1}. The Br-γ filter has a narrower bandwidth (2.13–2.18 μm), but a similar central wavelength (2.15 μm) compared the Ks filter (1.95–2.34 μm; 2.15 μm) and allows for longer integration times before saturation. A three-point dither pattern was utilized to avoid the noisier lower left quadrant of the NIRC2 array. The three-point dither pattern was observed three times with two coadds and a 30-second integration time per coadd for a total on-source exposure time of $3 \times 3 \times 2 \times 30\,{\rm s} = 540\,{\rm s}$.

The target star was measured with a resolution of $0\overset{''}{.}059$ (FWHM). No other stars were detected within the $10''$ field of view of the camera. In the Br-γ filter, the data are sensitive to stars that have K-band contrast of $\Delta{\rm K} = 4.3$ mag at a separation of $0\overset{''}{.}1$ and $\Delta{\rm K} = 7.49$ at $0\overset{''}{.}5$ from the central star. We estimate the sensitivities by injecting fake sources with an S/N of five into the final combined images at distances of $N \times$ FWHM from the central source, where N is an integer.

[11] We used the "resistant_mean" algorithm in the GSFC IDL library, http://idlastro.gsfc.nasa.gov/contents.html. Routines in this library were used for a number of other calculations in this work.
[12] http://exoplanetarchive.ipac.caltech.edu/

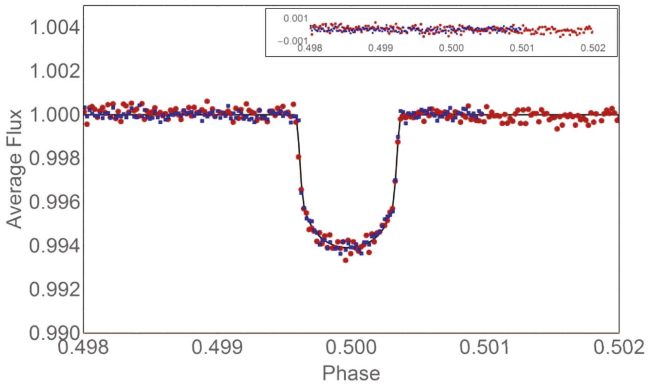

Figure 1. *Kepler* data from Quarters 6 and 17 have been normalized, detrended with a linear (Q6, red) or second order (Q17, blue) baseline, and phased around the period of the transit. The solid line shows a fit to these data using a model based on the EXOFAST routines (Eastman et al. 2013). The inset in the upper right shows residuals with respect to the fit.

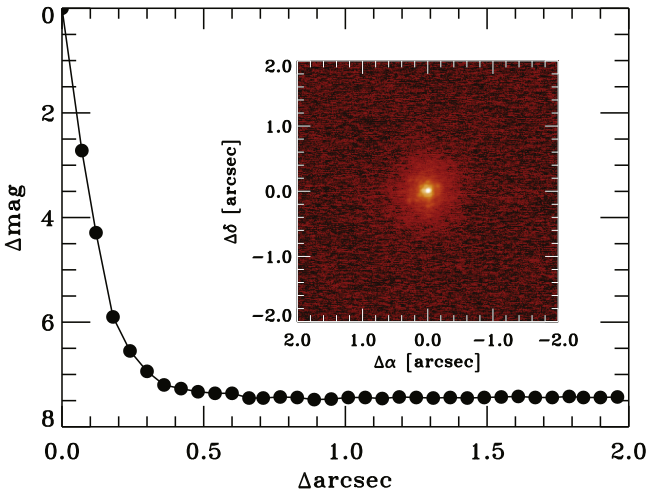

Figure 2. An image of Kepler-1654 obtained with the Keck II telescope in the narrow-band Br-γ filter shows no evidence for a companion within 4″ of the central star. The derived 5σ detection limits for the infrared imaging are also shown: differential magnitude as a function of angular separation from the primary star.

The 5σ sensitivities, as a function of radius from the star, are also shown in Figure 2.

There is a star 7″ northwest of Kepler-1654 that was outside of the field of view of the NIRC2 observations. However, this star is clearly resolved in 2MASS and is a separate star in the *Kepler* Input Catalog (KIC 8410692). The KIC photometry of KIC 8410692 (KepMag = 17.64 mag) indicates that the star has an effective temperature and a surface gravity of $T_{\rm eff} = 6111$ K and $\log g = 4.35$, making the star a main sequence F dwarf at a distance of about 4 kpc, and, thus, not a bound companion to Kepler-1654. The *Kepler* photometric aperture is oriented such that the background star is not included in the aperture in quarters 6 and 17 when the transits were observed, and the photocentric position remains centered on the Kepler-1654 during the transit, indicating that the transit occurs around the Kepler-1654 and not the background star. Further, at 50× fainter than Kepler-1654 the photometric blending of the background star (if the entire stellar profile were inside the photometric aperture) would only dilute the observed transit, and, hence, the derived planetary radius, by <1% (Ciardi et al. 2015).

3.2. Keck HIRES Spectroscopy

We obtained spectra of Kepler-1654 using the HIRES instrument (Vogt et al. 1994) at the W. M. Keck Observatory. Observations and data reduction followed the usual methods of the California Planet Search (CPS; Howard et al. 2010). A spectrum obtained with a 15-minute exposure on 2014 September 14 without the iodine cell was used for spectral typing (Figure 3). The spectral synthesis modeling program "SpecMatch" (Petigura 2015) has been calibrated with asteroseismology stars and yielded values of $T_{\rm eff}$, $\log g$, and [Fe/H] with formal uncertainties of 70 K, 0.06 dex, and 0.06 dex, respectively (Table 1). These parameters show the star is a slowly rotating, G5 main sequence star, perhaps beginning to evolve off the main sequence. The Ca H&K lines show no emission reversal implying a stellar age greater than ∼5 Gyr. An analysis looking for secondary spectra in the HIRES spectrum of Kepler-1654 found no companions brighter than 1% of the primary (Kolbl et al. 2015). These stellar values are similar to those cited in (Foreman-Mackey et al. 2016): our spectroscopically derived values of ($T_{\rm eff}$, R_*) = (5580 ± 70 K, 1.18 ± 0.03 $R_\odot$) versus (5918 ± 160 K, $1.0^{+0.35}_{-0.16}$ $R_\odot$) for Foreman-Mackey's values. We adopt our stellar values in this analysis (Tables 1 and 2).

We collected 18 RV measurements between 2014 September 07 and 2017 March 30. An iodine cell was used for each observation as a wavelength calibrator and point-spread function reference. Each spectrum spanned wavelengths from 3600 to 8000 Å with a spectral resolution of $R = 60000$ and typical S/N per pixel of 100–200. The "C2" decker (0.″87 × 14″ slit) provided spectral resolution $R \sim 55000$ and allowed for the sky background to be measured and subtracted. An exposure meter was used to automatically terminate exposures after reaching a target S/N per pixel at 550 nm. The standard CPS Doppler pipeline was used to measure RVs (Marcy & Butler 1992; Howard et al. 2009). RV measurements are listed in Table 3. These values are consistent with the transit interpretation, showing variations of <10 m s^{-1}, ruling out definitively the false alarm possibility of an eclipsing binary which would show RV variations of a few km s^{-1} on this timescale.

4. Analysis of the Transit and RV Observations

4.1. Properties of the Transiting Planet Kepler-1654b

First, it is important to confirm that this system truly represents a giant transiting planet. We used the VESPA tool to estimate (Morton 2012, 2015) the probability that this signal represents an astrophysical false positive. As inputs, we used the light curve shown in Figure 1, the stellar parameters listed in Table 1 along with *gri* photometry from APASS, the NIRC2 contrast curve described in Section 3.2, the Keck/HIRES limit on secondary spectra of Δmag < 5, and an upper limit on any secondary eclipse of 2×10^{-4}. The most likely false-positive configuration is that of a blended eclipsing binary, but this scenario is roughly 20000 times less likely than the planetary scenario. The resulting false-positive probability is 6.2×10^{-5}, more than sufficient to validate Kepler-1654b as a transiting planet. Foreman-Mackey et al. (2016) cited a false alarm rate due to eclipsing binaries of 0.05 based on statistical estimates of the contamination by background objects. Our much higher confidence level is due the follow-up observations, which gave direct and sensitive limits on stellar companions as well as

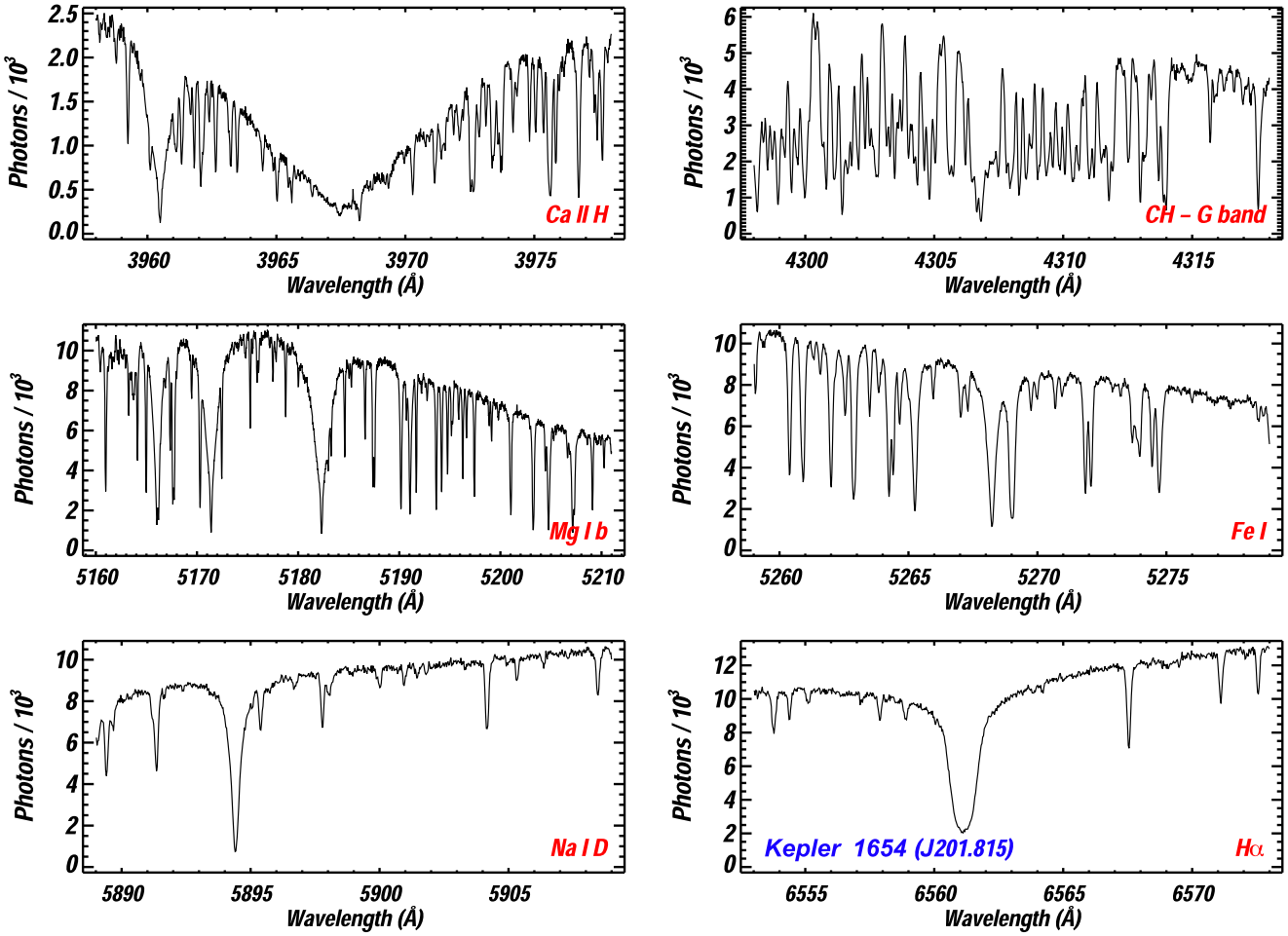

Figure 3. Spectra from the HIRES instrument on the Keck telescope. The top left panel shows a portion of the spectrum near the Ca H&K lines and the lack of an emission reversal implies a stellar age greater than ∼5 Gyr. The middle left and bottom right panels show lines near the Mg b triplet and H-α which look normal for a mid-G star with narrow lines.

taking advantage of improved stellar parameters. It is on this basis that we suggest Kepler-1654b (née KIC 8410697b) should be regarded as a fully confirmed *Kepler* object.

To determine the properties of the transiting companion, we used the EXOFAST transit analysis routine (Eastman et al. 2013) using stellar properties derived from the Keck data as priors plus the transit light curves as input.[13] We ran EXOFAST in its full MCMC mode with the eccentricity set to zero with the presented in Table 2 and shown in Figure 1. With 715 data points in the two observed transits, the χ^2 of the fit was 692.5 and the rms of the residuals was 0.00024 as shown in the figure. The various fitted parameters are astrophysically reasonable. For example, the derived limb-darkening coefficients of 0.40 ± 0.02 and 0.20 ± 0.03 are consistent with values appropriate to the stellar properties (Claret & Bloemen 2011). The EXOFAST fit shows the planet to be a Jupiter-sized object, 0.82 $R_{\rm Jup}$, in a 2.03 au orbit. At this location, the equilibrium temperature of the planet is 206 K assuming an albedo of zero.

Finally, we conducted a separate fit to the transit light curve using the BATMAN software package (Kreidberg 2015). All light curve parameters from this analysis agree with those in Table 2 to within 1σ. Using our posterior distributions, we computed the posterior of the stellar density under the assumption of a circular orbit (Seager & Mallén-Ornelas 2003). With the stellar density derived from our spectroscopic analysis, we then used the density posterior to investigate the photoeccentric effect (Dawson et al. 2012). The photoeccentric effect allows a direct and independent constraint on a transiting planet's orbital eccentricity through the observable impact of any non-zero orbital eccentricity on the transit light curve. Our analysis shows a preference for non-zero orbital eccentricity: we find $e = 0.3^{+0.3}_{-0.1}$, consistent with the weakly non-zero estimate from EXOFAST when run with eccentricity as a free parameter, $0.26^{+0.21}_{-0.11}$ (Table 2). The BATMAN analysis sets a lower limit on the eccentricity of $e > 0.06$ at 99.7% confidence. Thus, like most other giant, long-period exoplanets known from RV surveys, Kepler-1654b may also have an orbital eccentricity greater than that of Jupiter and Saturn. Finally, we note our derived planet values are consistent with those derived by Foreman-Mackey et al. (2016), e.g., $R_p = 0.82 \pm 0.06$ versus 0.70 ± 0.1 for (Foreman-Mackey et al. 2016).

4.2. Precision RV: Constraining Kepler-1654b

Although our RV measurements have helped to confirm the planetary nature of Kepler-1654b, our goal of determining the

[13] We used the implementation of EXOFAST available at the NASA Exoplanet Science Institute: https://exoplanetarchive.ipac.caltech.edu/cgi-bin/ExoFAST/nph-exofast.

Table 2
Median Values and 68% Confidence Interval for EXOFAST[a]

Parameter	Units	Value
Stellar Parameters:		
M_*	Mass ($M_\odot$)	$1.011^{+0.056}_{-0.052}$
R_*	Radius ($R_\odot$)	$1.179^{+0.026}_{-0.023}$
L_*	Luminosity ($L_\odot$)	$1.23^{+0.12}_{-0.11}$
ρ_*	Density (cgs)	$0.876^{+0.015}_{-0.033}$
$\log(g_*)$	Surface gravity (cgs)	$4.3001^{+0.0099}_{-0.012}$
$T_{\rm eff}$	Effective temperature (K)	5597^{+95}_{-93}
[Fe/H]	Metallicity	$-0.088^{+0.097}_{-0.095}$
Planetary Parameters:		
P	Period (days)	$1047.8356^{+0.0018}_{-0.0019}$
a	Semimajor axis (au)	$2.026^{+0.037}_{-0.035}$
R_P	Radius (R_J)	$0.819^{+0.019}_{-0.017}$
T_{eq}	Equilibrium Temperature (K)	$206.0^{+3.7}_{-3.5}$
$\langle F \rangle$	Incident flux (10^9 erg s^{-1} cm^{-2})	$0.000408^{+0.000030}_{-0.000027}$
Primary Transit Parameters:		
T_C	Time of transit (BJD_{TDB})	$2455375.1341^{+0.0014}_{-0.0015}$
R_P/R_*	Radius of planet in stellar radii	$0.07138^{+0.00033}_{-0.00032}$
a/R_*	Semimajor axis in stellar radii	$370.3^{+2.2}_{-4.7}$
u_1	linear limb-darkening coeff	$0.401^{+0.024}_{-0.025}$
u_2	quadratic limb-darkening coeff	0.205 ± 0.034
i	Inclination (degrees)	$89.982^{+0.012}_{-0.017}$
b	Impact Parameter	$0.114^{+0.11}_{-0.079}$
δ	Transit depth	$0.005096^{+0.000047}_{-0.000045}$
$T_{\rm FWHM}$	FWHM duration (days)	$0.8933^{+0.0038}_{-0.0053}$
τ	Ingress/egress duration (days)	$0.06463^{+0.0023}_{-0.00072}$
T_{14}	Total duration (days)	$0.9580^{+0.0035}_{-0.0039}$
P_T	A priori non-grazing transit prob	$0.002508^{+0.000032}_{-0.000015}$
$P_{T,G}$	A priori transit prob	$0.002893^{+0.000038}_{-0.000017}$
F_0	Baseline flux	$1.0000036^{+0.0000089}_{-0.0000087}$
Secondary Eclipse Parameters:		
T_S	Time of eclipse (BJD_{TDB})	$2455899.05191 \pm 0.00091$
From EXOFAST run with non-zero eccentricity		
e	Eccentricity	$0.26^{+0.21}_{-0.11}$
ω_*	Argument of periastron (degrees)	81^{+73}_{-71}

Note.
[a] Parameters derived with eccentricity forced to zero except as noted.

Table 3
Keck HIRES Data for Kepler-1654

JD Date	Velocity (m s^{-1})	σVel (m s^{-1})
2456907.899441	4.61	3.42
2457061.166912	13.98	5.52
2457062.168017	−1.34	5.19
2457151.051283	−7.03	3.13
2457180.021422	−0.33	3.78
2457201.026295	−16.67	3.90
2457203.095994	11.25	4.68
2457211.936684	9.66	3.31
2457229.053345	−2.74	3.63
2457326.714999	−3.32	3.21
2457353.692574	8.66	3.21
2457354.729928	7.67	4.20
2457478.135425	−2.43	3.72
2457521.001943	−8.54	3.06
2457601.046180	−7.80	5.64
2457620.898209	7.04	3.33
2457672.824144	2.84	3.76
2457830.140368	−19.56	3.38

Table 4
Model Comparison

Statistic	0 planets	1 planet
$N_{\rm data}$ (number of measurements)	18	18
$N_{\rm free}$ (number of free parameters)	2	3
rms (rms of residuals in m s^{-1})	9.12	8.88
χ^2 (assuming no jitter)	69.91	67.22
χ^2_ν (assuming no jitter)	4.37	4.48
$\ln \mathcal{L}$ (natural log of the likelihood)	−65.29	−64.87
BIC (Bayesian information criterion)	135.48	135.62

Table 5
MCMC Posteriors

Parameter	Value	Units
Modified MCMC Step Parameters		
$\sqrt{e}\cos\omega_b$	$\equiv 0.0$	
$\sqrt{e}\sin\omega_b$	$\equiv 0.0$	
Orbital Parameters		
P_b	$\equiv 1047.8363$	days
$T\mathrm{conj_b}$	$\equiv 2455375.133$	JD
e_b	$\equiv 0.0$	
ω_b	$\equiv 0.0$	degrees
K_b	$2.7^{+3.2}_{-3.3}$	m s^{-1}
Other Parameters		
γ (RV offset)	-1.1 ± 2.6	m s^{-1}
σ (jitter)	$9.1^{+2.3}_{-1.7}$	m s^{-1}

mass of the transiting planet has not yet been achieved. We analyzed the 18 HIRES RV measurements (Table 3), which span 2.5 years, using the open source Python package `RadVel` (Fulton et al. 2018). We adopt an RV model consisting of a single Keplerian, with orbital period and phase fixed at the known values and assuming an eccentricity of zero. The model includes a constant RV offset, γ, and a "jitter" term σ representing astrophysical and instrumental noise. The MCMC analysis (Tables 4 and 5) yields an estimate of the semi-amplitude $K_b = 2.7^{+3.2}_{-3.3}$ m s^{-1} which corresponds to $43 \pm 52\,M_\oplus$ ($0.13 \pm 0.16\,M_{\rm Jup}$), or a 3σ upper limit of $<156\,M_\oplus$ ($< 0.49\,M_{\rm Jup}$). Figure 4 shows the RV data plotted along with the best-fit model, while Figures 5 and 6 show the posterior distributions of the model parameters. A zero-planet model is favored on the basis of the Bayesian Information Criterion (Table 4), consistent with a non-detection.

What level of signal might we expect to find on the basis of a planet of radius 0.82 $R_{\rm Jup}$? The radius–mass data shown in Figure 3 of Howard (2013) suggest that with a radius of 9.2 $R_\oplus$, Kepler-1654b should have a mass in the range of 50–100 $M_\oplus$. Wolfgang et al. (2016) give a number of radius–mass relationships for planets with $R < 4\,R_\oplus$ (somewhat smaller than Kepler-1654b) and their Method-1 yields a mass estimate of 58 $M_\oplus$, which falls within the Howard (2013) range. These masses correspond to RV semi-amplitudes of 3–6 m s^{-1} which our RV data only begin to constrain.

The corresponding upper limit to the bulk density is <1.2 g cm^{-3}. As shown in Figure 7, the limit to Kepler-1654b's density sits close to Saturn's in the Mass–Radius–Density parameter space. Our RV observations rule out the most massive planets but are consistent with the distribution of planetary

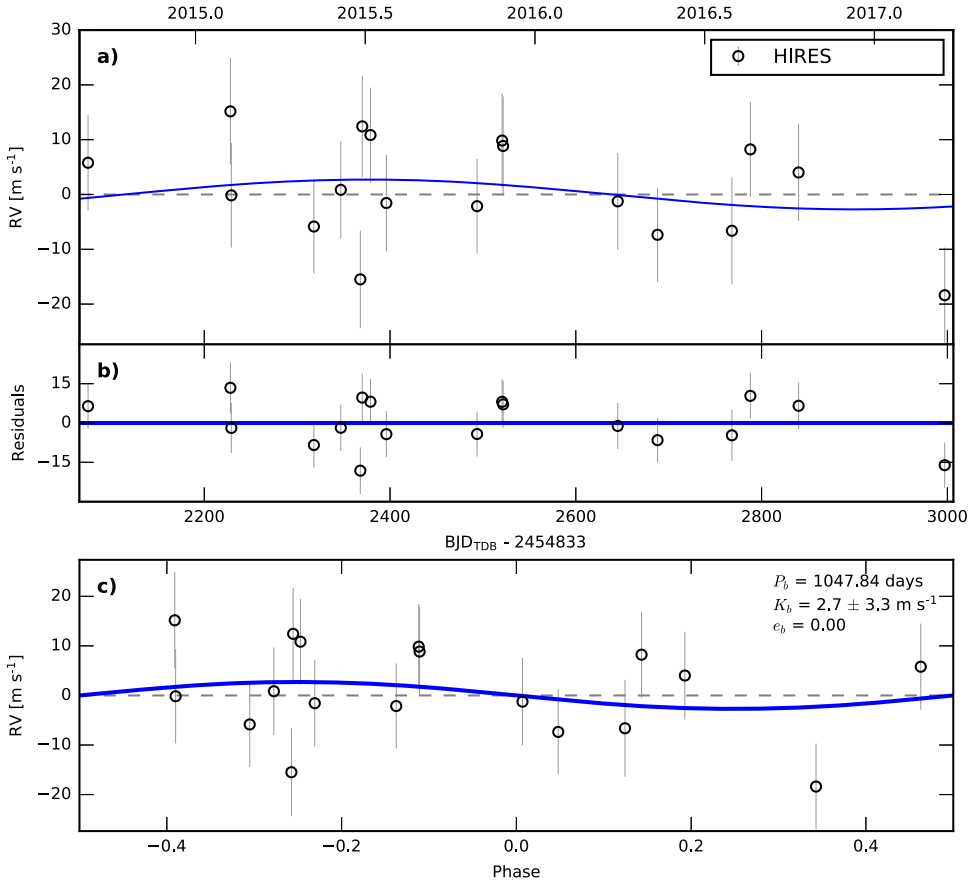

Figure 4. Best-fit one-planet Keplerian orbital model for Kepler-1654b. The maximum likelihood model is plotted while the orbital parameters listed in Table 5 are the median values of the posterior distributions. The thin blue line is the best-fit one-planet model. We add in quadrature the RV jitter term(s) listed in Table 5 with the measurement uncertainties for all RVs. (b) Residuals to the best-fit one-planet model. (c) RVs phase-folded to the ephemeris of planet b. The small point colors and symbols are the same as in panel (a). The phase-folded model for planet b is shown as the blue line.

densities in this radius range. Continuing RV observations will eventually yield a mass for the transiting system.

We can use our RV data to explore the upper limit to the mass of the any interior planet. With a 1σ rms residual of $9.1\,\mathrm{m\,s^{-1}}$ (Table 4) and 18 observations, we can set a 3σ upper limit to the RV semi-amplitude any interior planet (transiting or not) of $K = 3 \times 9.1/\sqrt{18} = 6.4\,\mathrm{m\,s^{-1}}$ for a low inclination planet where K is given by:

$$K = \frac{28.4\ \mathrm{m\ s^{-1}}}{\sqrt{1-e^2}} M_{\rm pl}\ \sin(i)\ M_*^{-2/3}\ P^{-1/3} \qquad (2)$$

with the planet mass with the planet mass in Jupiter units, the stellar mass in solar units and the period in years (Lovis & Fischer 2010). Assuming $\sin(i) = 1$ for a system with at least one transiting planet, a stellar mass of $1\,M_\odot$, and $e = 0$, the HIRES observations set a mass limit for any additional planet of $M_{\rm pl} < 0.23 P_{\rm yr}^{1/3}\,M_{\rm Jup}$.

Of primary importance will be to follow the Kepler-1654 system with additional RV monitoring to determine the planet's mass. New imaging and RV observations are planned to investigate the new long-period systems found by Foreman-Mackey et al. (2016).

5. Characterizing the Atmosphere of Temperate Gas Giants

Kepler-1654b is representative of the few temperate, transiting gas giants available for atmospheric characterization. We investigated whether this system might be promising for spectroscopy with the *Hubble* (*HST*) and *James Webb Space Telescopes* (*JWST*; Beichman et al. 2014). Kepler-1654b and others like it as described in Wang et al. (2015) and Kipping et al. (2016) (Table 7) will be the coolest gas planets (~200 K) for which we will be able to probe atmospheric composition and physical characteristics. Comparisons to planets in our own solar system will be particularly valuable.

Kepler-1654b is cold for a transiting planet. The strength of absorption features in transmission spectra are proportional to a planet's atmospheric scale height, and that scale height is proportional to atmospheric temperature. Therefore, the low temperature of the planet produces a small amplitude transmission spectrum. This plus the relative faintness of Kepler-16547 itself limits the signal-to-noise of its transmission spectrum. On the plus side, the long duration of these events enhances the sensitivity for measurements of trace atomic and molecular species in the 1–5 μm band. Sample spectra in the visible and near-IR for Kepler-1654b are shown in Figure 8.

We have simulated *JWST* NIRSpec prism spectra for a single transit of this system and show the results in Figure 8. These spectra were computed using the method described in Greene et al. (2016) and use Nextgen (Hauschildt et al. 1999) stellar models with the $T_{\rm eff}$ and log g of Kepler-1654 (Table 1) and our atmospheric transmission models of Kepler-1654b. We model the atmosphere by solving radiative and chemical equilibrium and also include condensation of water when supersaturation is reached. Three atmospheric models with $g = 10\,\mathrm{m\,s^{-2}}$ with

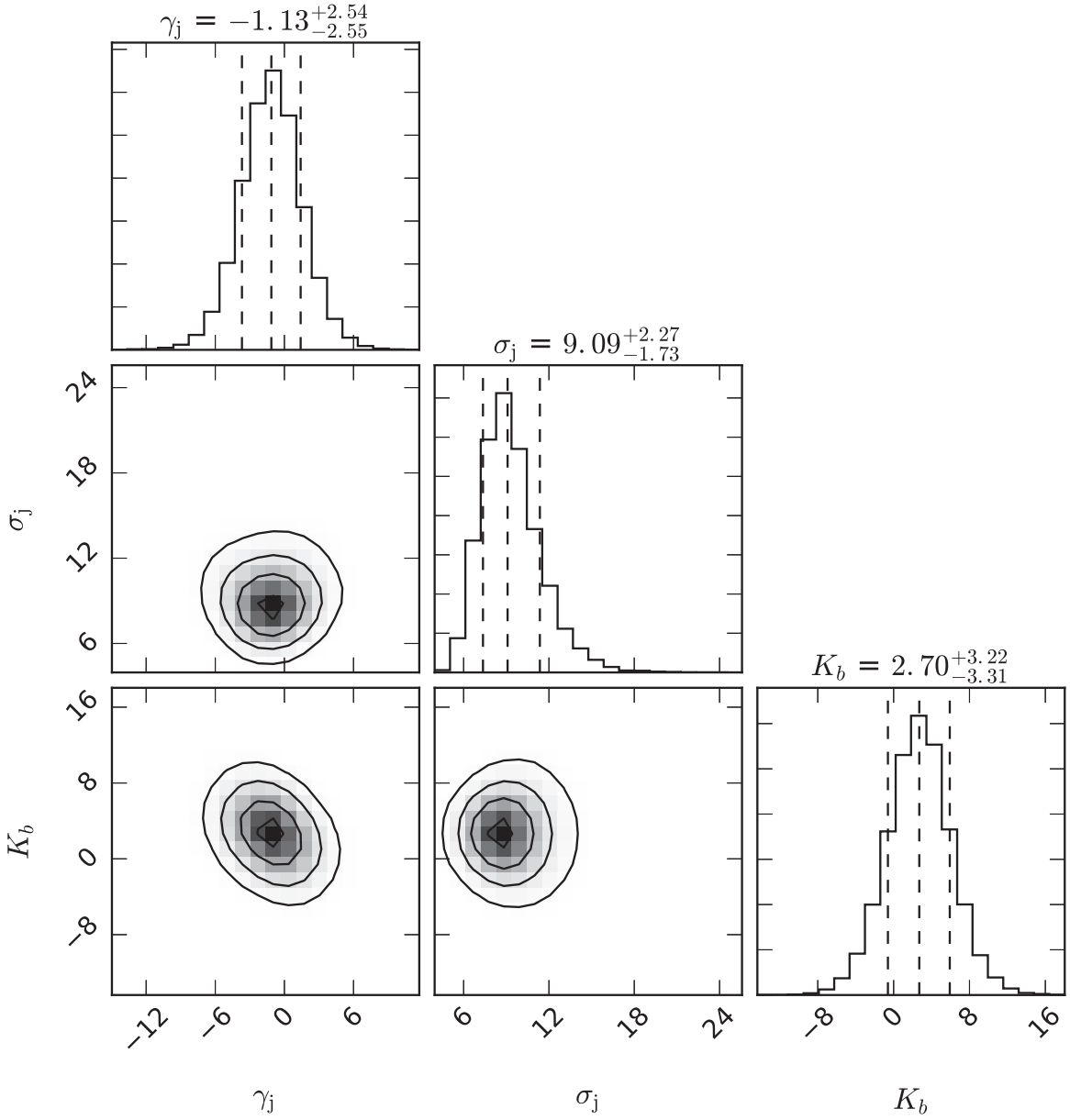

Figure 5. Posterior distributions for all free parameters in the RV fit.

and without clouds and $g = 25\,\mathrm{m\,s^{-2}}$ without clouds are shown in the top panel of Figure 8(a). We computed signals in photo-electrons using the apparent stellar magnitude of Kepler-1654 in the relevant bands, 18 hr integration time on transit, an additional 18 hr on the star, the 25 m^2 collecting area of *JWST*, and NIRSPEC prism resolving power and system transmission values kindly provided by the NIRSpec team (S. Birkmann 2018, private communication). The resultant 1σ noise values are on the order of 15 ppm when binned to $R = 10$, lower than the best values achieved with *HST* WFC3 G141 observations (e.g., Kreidberg et al. 2014a). It is uncertain whether *JWST* NIRSpec or other *JWST* instruments will achieve such low noise levels, so Figure 8 represents the best performance that *JWST* is likely to achieve on a single transit observation of this system.

A second scenario for the planet's atmosphere includes enhanced transmission spectral features from a heated stratosphere (Figure 8(b)). Our models predict that the transmission spectra are sensitive to the scale height above a cloud deck at 0.1–1.0 bar. If the temperature above the cloud deck is substantially higher than the equilibrium temperature (~200 K) of the planet, the strength of the absorption features will be proportionally larger (Figure 8). Such a stratosphere commonly exists in all giant planets in the solar system, and has recently been detected in one hot exoplanet (Evans et al. 2017), although the degree of heating with respect to their equilibrium temperatures differs from planet to planet. Figure 8(b) shows models with and without a heated stratosphere (HS) and two levels of metallicity, solar and 10× solar. The effect of stratospheric heating is much stronger than enhanced metallicity.

Figure 8 shows that *JWST* could detect the strong CH_4 features at 2.3 and 3.4 μm at low-to-moderate confidence in several models. We expect that spectral retrieval algorithms (e.g., Line et al. 2013a) will likely provide a higher confidence detection of CH_4, as such methods combine information on all

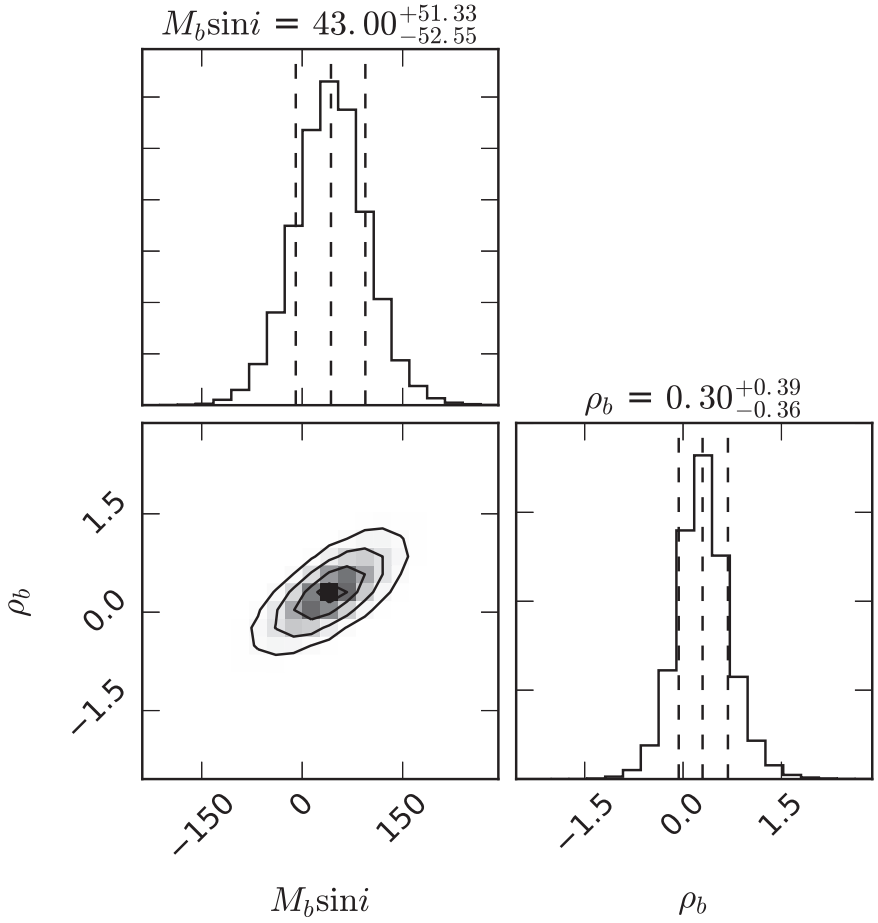

Figure 6. Posterior distributions for all derived parameters.

Table 6
Predicted Epochs of Future Transits for Kepler-1654b (UT)

Orbit	Transit Midpoint (BJD)	Transit Midpoint (UT)
0	2,455,375.1341 ± 0.0014	2010 Jun 27 15:13:06 ± 120 (s)
1	2,456,422.9697 ± 0.0024	2013 May 10 11:16:22 ± 200 (s)
2	2,457,470.8053 ± 0.0040	2016 Mar 23 07:19:38 ± 350 (s)
3	2,458,518.6409 ± 0.0059	2019 Feb 4 03:22:54 ± 510 (s)
4	2,459,566.4765 ± 0.0077	2021 Dec 17 23:26:10 ± 670 (s)
5	**2,460,614.3121 ± 0.0096**	**2024 Oct 30 19:29:25 ± 830 (s)**
6	2,461,662.1477 ± 0.0115	2027 Sep 13 15:32:41.3 ± 990 (s)
7	2,462,709.9833 ± 0.0134	2030 Jul 27 11:35:57.1 ± 1,160 (s)
8	2,463,757.8189 ± 0.0153	2033 Jun 9 07:39:13.0 ± 1,320 (s)

Note. These predicted transit midpoints assume no offsets due to interactions with other bodies in the system (Transit Timing Variations, TTVs). The bold entry for 2024 October 30 is nominally the first one observable by *JWST* and occurs at the edge of the *JWST* observability window.

features in the observed spectrum. We do not expect *HST* observations to yield detections of CH_4 or other features in the model spectra. The smaller aperture of *HST* will produce lower S/N in the 1.1–1.7 μm passband of its WFC3 G141 instrument mode than for *JWST* NIRSpec. The transmission models show no spectral absorption features and only modest Raleigh slopes at wavelengths shorter than $\lambda = 600$ nm (*JWST*/NIRSpec's lower cutoff), so shorter wavelength *HST* observations will also not be able to constrain the planet's atmospheric properties.

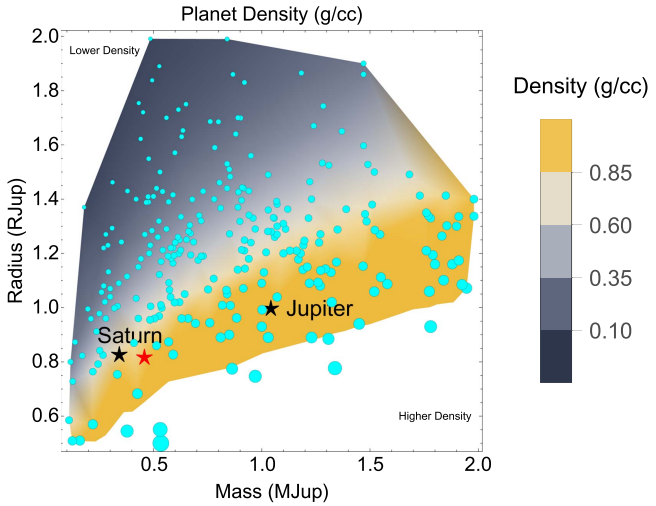

Figure 7. The distribution of bulk density in g cm^{-3} for planets with radii in the range of 0.5–2 $R_{\rm Jup}$ based on data for over 250 transiting planets with well determined mass and radius measurements (cyan points). The color scale shows bulk densities from 0.1 to >1 g cm^{-3} and shows the fall-off in bulk density for more massive planets (Howard et al. 2013). The positions of Saturn, Jupiter, and the upper limit to Kepler-1654b (red star) are indicated. The point size is proportional to the planet's density.

The *JWST* NIRSpec prism spectra could certainly detect the spectral features in the heated stratosphere models.

Finally, we put Kepler-1654b into the context of other long-period transiting systems suitable for observation by *JWST*.

Table 7
Properties of Long-period Transiting Planets

Planet Name	Period (days)	R_{pl} (R_{Jup})	Depth (ppm)	Duration (days)	Ks (mag)	WISE2 (mag)	S/N[a] (Ks)	S/N[a] (*W2*)	T_{pl} (K)	First *JWST*
Kepler-167e (1)	1070	0.91	16,224	0.67	11.83	11.84	407	213	140	2024 Oct 25
PH2b/Kepler 86b (9)	280	0.90	8,589	0.44	11.12	11.14	242	126	284	2020 Oct 28
Kepler-553c (6)	330	1.00	14,549	0.51	13.06	12.88	180	103	234	2019 Jun 08
Kepler-1654b[b] (2)	1410	0.82	5095	0.89	11.92	11.93	141	74	177	2024 Oct 30 (11)
Kepler-421b (4)	700	0.37	2510	0.66	11.54	11.49	71	38	177	2025 Oct 10
Kepler-1647b (3)	1110	1.06	3687	0.41	12.00	11.90	67	37	255	2021 Aug 02
Kepler-1625b (6)	290	0.54	3489	0.79	13.92	13.92 (12)	36	19	275	2019 May 26
KIC 9663113b (5)	570	0.41	1669	0.83	12.50	12.46	34	18	244	2020 Oct 23
Kepler-1536b (6)	360	0.28	1840	0.54	12.55	12.54	30	16	176	2019 May 12
KIC 10525077b (5)	850	0.49	2489	0.83	13.75	13.80	29	15	211	2019 Apr 11
Kepler-1630b (6)	510	0.20	1009	0.35	11.80	11.71	18	10	165	2019 Jul 15
Kepler-22b (10)	290	0.21	493	0.31	10.15	10.15	18	10	272	2019 Sep 08
Kepler-1634b (6)	370	0.29	1080	0.47	12.72	12.68	15	8	238	2019 Aug 02
Kepler-150f (7)	640	0.33	1259	0.56	13.37	13.37	14	7	207	2024 May 09
Kepler-1635b (6)	470	0.33	1540	0.56	13.90	13.90	14	7	212	2020 Jun 12
Kepler-1600b (6)	390	0.28	1219	0.41	13.90	13.88	9	5	218	2019 Oct 06
Kepler-1632b (6)	450	0.22	360	0.53	11.66	11.64	9	5	281	2020 May 15
Kepler-1636b (6)	430	0.29	840	0.74	14.23	14.23 (12)	7	4	255	2023 May 23

Note. (1) Kipping et al. (2016), (2) This work; (3) Circumbinary planet with multiple transits Kostov et al. (2016), (4) Kipping et al. (2014), (5) Wang et al. (2015), (6) Morton et al. (2016), (7) Schmitt et al. (2017). (8) Jenkins et al. (2015). (9) Wang et al. (2013). (10) Borucki et al. (2012). (11) This transit is just at the edge of the *JWST* observability window based on current knowledge. (12) Estimated from 2MASS.
[a] See the text for a description of the "Transit S/N" figure of merit in $R = 100$ spectral element.
[b] The bold entry refers to the planet identified in this paper.

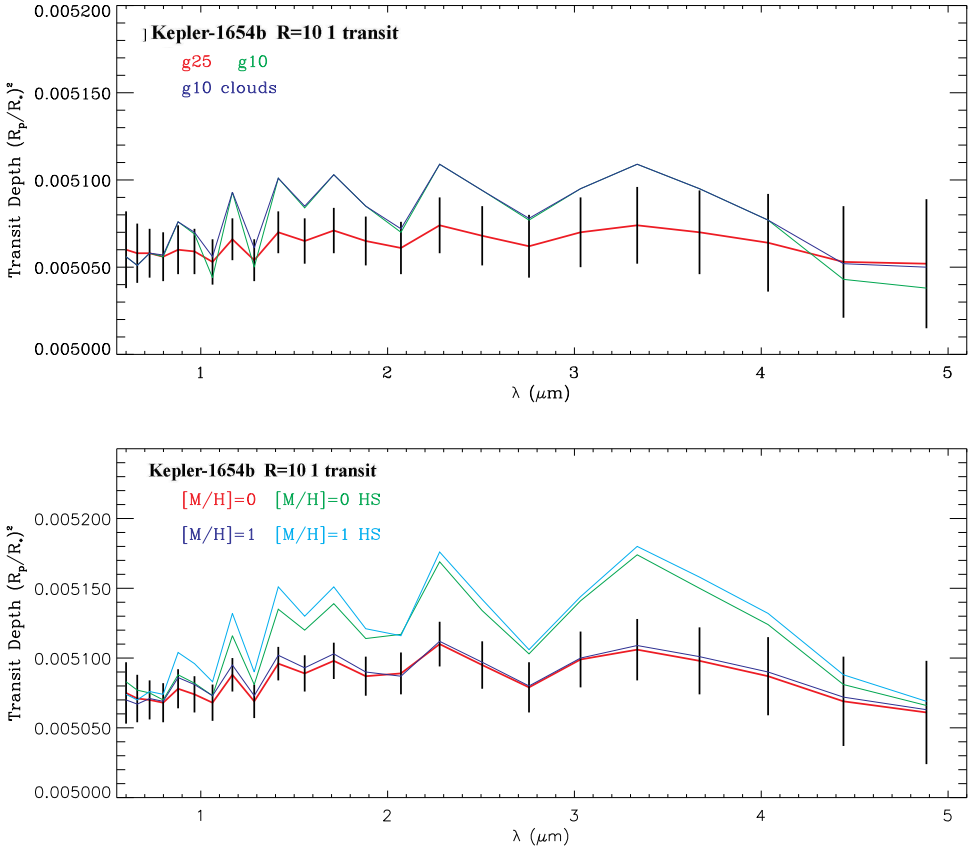

Figure 8. (Top) Simulated *JWST* NIRSpec prism spectrum of Kepler-1654b with uncertainties computed as described in Greene et al. (2016). Model spectra have been binned to $R = 10$ and are shown as solid colored curves. 1σ uncertainties were computed for a single 18.4 hr transit at $R = 10$ and are shown as error bars. Three atmospheric models with $g = 10$ m s^{-2} with and without clouds and $g = 25$ m s^{-2} without clouds appear in the top panel. The bottom panel shows $R = 10$ models and uncertainties for $g = 25$ m s^{-2} atmospheres with and without a heated stratosphere (HS) and two levels of metallicity, solar and 10× solar.

Table 7 gives data on 18 confirmed planets with radius $\geqslant 2\,R_{\oplus}$, orbital periods greater than 250 days and an equilibrium temperature[14] $T_{\rm pl} < 300$ K. We developed a figure of merit which takes into account the total number of stellar photons, denoted S, observed in a spectral element, $\Delta\nu$, in a time τ; the photon shot-noise, $\sigma = \sqrt{S}$; and the transit depth, α. The "Transit S/N" is defined as $\alpha S/\sigma = \alpha\sqrt{S}$ and is evaluated for stellar flux densities, F_{ν}, at K_s (2.2 μm) or *WISE W2* (4.6 μm) for a telescope with a collecting area $A = 25\,{\rm m}^2$, with an instrument of resolution $R = 100$ and efficiency $\eta = 0.25$, and in an integration time, τ, equal to the duration of a transit: $S = F_{\nu} A\eta\Delta\nu\,\tau/(h\nu)$. This figure of merit glosses over many details (Greene et al. 2016), but serves to rank these planets in terms of their suitability for transit spectroscopy. For planets with a temperature below 200 K, only Kepler-167e, which is a larger planet orbiting a smaller star (Kipping et al. 2016), has a "Transit S/N" larger than Kepler-1654b's. Other systems rank a factor of two or more lower, making Kepler-1654b a valuable target for future study. Of course, the atmospheric scale height which depends on the planet's temperature and surface gravity also affects the detectability of spectral signatures. But as only a few of these planets have RV-determined masses, we do not account for the effects of scale height here.

Table 6 and the last column of Table 7 highlight the challenge of actually observing these long-period planets. The long time between transits and *JWST*'s limited pointing windows can make scheduling difficult. *JWST*'s Sun avoidance restrictions determine when the $10^{\circ} \times 10^{\circ}$ *Kepler* field can be observed, nominally from early/mid-April to late-October/mid-November. Thus, for example, transits of Kepler-1654b and Kepler 167e will be observable only starting with the 2024 events based on extrapolations from the information in the *JWST* APT tool.

6. Conclusion

We have searched Q1-Q17 *Kepler* light curves of F and G stars not previously associated with confirmed or candidate planets or even with *Kepler* "Objects of Interest" and we were able to identify Kepler-1654b (originally KIC 8410697b), which shows two transits with a 1047 day period—one of the longest periods yet found in the *Kepler* survey. Subsequent AO and RV observations were able to rule out false positives and to characterize the planet and its host star. A fit to the combined transit curve plus RV data shows that orbiting this mature G5 star is a $0.82\,R_{\rm J}$ planet with a mass of $<0.5\,M_{\rm Jup}$. Transit spectroscopy with *JWST* of Kepler-1654b and similar objects will enable a careful study of planets whose physical states, e.g., a low equilibrium temperature of $\sim$200 K, most closely resemble those of the outer planets in our own solar system.

Some of the research described in this publication was carried out in part at the Jet Propulsion Laboratory, California Institute of Technology, under a contract with the National Aeronautics and Space Administration. This research has made use of the NASA/IPAC Infrared Science Archive (IRSA), the Keck Observatory Archive (KOA), and the NASA Exoplanet Archive, which are operated by the Jet Propulsion Laboratory, California Institute of Technology, under contract with the National Aeronautics and Space Administration. We used the implementation of EXOFAST available at the NASA Exoplanet Science Institute.

We are grateful to an anonymous referee for a careful reading of the manuscript, which led to a number of improvements. Some data presented herein were obtained at the W. M. Keck Observatory from telescope time allocated to the National Aeronautics and Space Administration through the agency's scientific partnership with the California Institute of Technology and the University of California. The Observatory was made possible by the generous financial support of the W. M. Keck Foundation. The authors wish to recognize and acknowledge the very significant cultural role and reverence that the summit of Maunakea has always had within the indigenous Hawaiian community. We are most fortunate to have the opportunity to conduct observations from this mountain. Finally, H.G. acknowledges support of a summer internship made possible by Caltech and JPL.

[14] We adopt an illustrative equilibrium temperature given by $T_{\rm pl} = 265 L^{0.25} d^{-0.5}$ K for a planet located at d(au) from a star of luminosity, $L(L_{\odot})$.

ORCID iDs

H. Isaacson https://orcid.org/0000-0002-0531-1073
G. M. Marcy https://orcid.org/0000-0002-2909-0113
E. Sinukoff https://orcid.org/0000-0002-5658-0601
J. J. Fortney https://orcid.org/0000-0002-9843-4354
A. W. Howard https://orcid.org/0000-0001-8638-0320
E. A. Petigura https://orcid.org/0000-0003-0967-2893

References

Batalha, N. M., Rowe, J. F., Bryson, S. T., et al. 2013, ApJS, 204, 24
Beichman, C., Benneke, B., Knutson, H., et al. 2014, PASP, 126, 1134
Borucki, W. J., Koch, D., Basri, G., et al. 2010, Sci, 327, 977
Borucki, W. J., Koch, D. G., Batalha, N., et al. 2012, ApJ, 745, 120
Brown, T. M., Latham, D. W., Everett, M. E., & Esquerdo, G. A. 2011, AJ, 142, 112
Ciardi, D. R., Beichman, C. A., Horch, E. P., & Howell, S. B. 2015, ApJ, 805, 16
Claret, A., & Bloemen, S. 2011, A&A, 529, A75
Dawson, R. I., Johnson, J. A., Morton, T. D., et al. 2012, ApJ, 761, 163
Eastman, J., Gaudi, B. S., & Agol, E. 2013, PASP, 125, 83
Evans, T. M., Sing, D. K., Kataria, T., et al. 2017, Natur, 548, 58
Foreman-Mackey, D., Morton, T. D., Hogg, D. W., Agol, E., & Schölkopf, B. 2016, AJ, 152, 206
Fulton, B. J., Petigura, E. A., Blunt, S., & Sinukoff, E. 2018, arXiv:1801.01947
Greene, T. P., Line, M. R., Montero, C., et al. 2016, ApJ, 817, 17
Hauschildt, P. H., Allard, F., & Baron, E. 1999, ApJ, 512, 377
Howard, A. W. 2013, Sci, 340, 572
Howard, A. W., Johnson, J. A., Marcy, G. W., et al. 2009, ApJ, 696, 75
Howard, A. W., Johnson, J. A., Marcy, G. W., et al. 2010, ApJ, 721, 1467
Howard, A. W., Sanchis-Ojeda, R., Marcy, G. W., et al. 2013, Natur, 503, 381
Huber, D., Silva Aguirre, V., Matthews, J. M., et al. 2014, ApJS, 211, 2
Jenkins, J. M., Caldwell, D. A., Chandrasekaran, H., et al. 2010, ApJL, 713, L87
Jenkins, J. M., Twicken, J. D., Batalha, N. M., et al. 2015, AJ, 150, 56
Kipping, D. M., Torres, G., Buchhave, L. A., et al. 2014, ApJ, 795, 25
Kipping, D. M., Torres, G., Henze, C., et al. 2016, ApJ, 820, 112
Kolbl, R., Marcy, G. W., Isaacson, H., & Howard, A. W. 2015, AJ, 149, 18
Kostov, V. B., Orosz, J. A., Welsh, W. F., et al. 2016, ApJ, 827, 86
Kreidberg, L. 2015, PASP, 127, 1161
Kreidberg, L., Bean, J. L., Désert, J.-M., et al. 2014, Natur, 505, 69
Line, M. R., Wolf, A. S., Zhang, X., et al. 2013, ApJ, 775, 137
Lovis, C., & Fischer, D. 2010, in Exoplanets, ed. S. Seager (Tucson, AZ: Univ. Arizona Press), 27
Marcy, G. W., & Butler, R. P. 1992, PASP, 104, 270
Marcy, G. W., Isaacson, H., Howard, A. W., et al. 2014, ApJS, 210, 20
Morton, T. D. 2012, ApJ, 761, 6

Morton, T. D. 2015, VESPA: False positive probabilities calculator, Astrophysics Source Code Library, ascl:1503.011
Morton, T. D., Bryson, S. T., Coughlin, J. L., et al. 2016, ApJ, 822, 86
Petigura, E. A. 2015, PhD thesis, Univ. California, Berkeley
Santerne, A., Fressin, F., Díaz, R. F., et al. 2013, A&A, 557, A139
Schmitt, J. R., Jenkins, J. M., & Fischer, D. A. 2017, AJ, 153, 180
Seager, S., & Mallén-Ornelas, G. 2003, ApJ, 585, 1038
Vogt, S. S., Allen, S. L., Bigelow, B. C., et al. 1994, Proc. SPIE, 2198, 362
Wang, J., Fischer, D. A., Barclay, T., et al. 2013, ApJ, 776, 10
Wang, J., Fischer, D. A., Barclay, T., et al. 2015, ApJ, 815, 127
Wolfgang, A., Rogers, L. A., & Ford, E. B. 2016, ApJ, 825, 19